

Temporal 2D Reconstruction of Cell Nucleus from Fluorescence Confocal Microscopy Images with Anisotropic Filtering

Isabel Rodrigues^{1,2} and João Sanches^{2,3}

Abstract—*Fluorescence Confocal Microscopy*(FCM) is nowadays one of the most important tools in biomedicine research. In fact, it makes possible to accurately study the dynamic processes occurring inside the cell and its nucleus by following the motion of fluorescent molecules along the time. Due to the small amount of acquired radiation and the huge optical and electronics amplification, the FCM images are usually corrupted by a severe type of Poisson noise. This noise may be even more damaging when very low intensity incident radiation is used to avoid *phototoxicity*.

In this paper a Bayesian algorithm is proposed to remove the Poisson *multiplicative* noise corrupting the FCM images. The observations are organized in a 3D tensor where each plane is one of the images acquired along the time of a cell using the *Fluorescence Loss In Photobleaching* (FLIP) technique. The method removes simultaneously the noise by considering different spatial and temporal correlations. This is done by using an anisotropic 3D filter that may be separately tuned in space and time dimensions.

Tests using synthetic and real data are described and presented to illustrate the application of the algorithm.

Index Terms—Denoising, Poisson, Bayesian, confocal microscopy, convex optimization.

I. INTRODUCTION

Confocal microscopy is known since the end of fifties. However, the most significant advances occurred during the last decade. The fluorescence confocal microscope has become one of the most powerful tools in medical and biological research [1] due to the improvement of the *laser scanning confocal microscope* (LSCM) [2], to the development of synthetic fluorescent probes and proteins and to the development of a wider spectrum of laser light sources coupled to highly accurate acoustic/optic controlled filters. The main advantage of the fluorescence confocal microscope over the traditional optical one consists on its capability to illuminate a thin plan of the specimen to be observed, collecting the light radiated from that plan and eliminating the out-of-focus information [2]. The illumination is provided by a highly focused laser beam and the observation is performed by rejecting all radiation but the one emitted by the fluorescence effect.

One difficulty arising in this modality of image microscopy is the *photobleaching* effect. This, phenomenon occurs when fluorophore permanently loses the ability to fluoresce, due to chemical reactions induced by the incident laser or by other surrounding molecules. This effect leads

to a decrease in the image intensity along the time and at space varying rates. When the acquisition is fast and the laser intensity is low this phenomenon is not relevant. But in long time acquisition processes or when high intensity lasers are used this effect must be considered. However, this undesirable effect may be used to study some dynamic processes occurring inside the cell [3].

A common technique employed to measure the molecular mobility and to study the dynamics in living cells is *Fluorescence Loss In Photobleaching* (FLIP). In this technique a small defined area is repeatedly bleached over time by a high intensity laser beam and the surrounding area is monitored for a decrease in the level of fluorescence. Any fraction of the cell connected to the area being bleached will gradually fade owing to the movement of bleached molecules into the region. In contrast, regions of the cell not connected to the bleached region will remain unaffected and continue to fluoresce. The FLIP technique can be used to assess whether or not a tagged bio-molecule moves to a particular area of the cell [4].

In this paper a denoising algorithm is proposed for FCM images where the FLIP technique is used. The goal is to study the process of RNA molecules synthesis inside the cell nucleus, namely, their flow along the time. These molecules are tagged with *Green Fluorescent Protein* (GFP) to be observed in the FCM images.

The denoising algorithm is formulated in the Bayesian framework where a Poisson distribution models the observation noise and a Gibbs distribution, with *log-quadratic* potential functions, regularizes the solution, defining the field to be estimated as a *Markov Random Field* (MRF). This *log-quadratic* potential functions have shown to be more appropriated to deal with this type of optimization problems in R_+^N [5]. The regularization is performed in the image space and in time (time courses) using different prior parameters. The denoising iterative algorithm involves an anisotropic 3D filtering process to cope with the different smoothing effects performed in the space and time dimensions.

Tests using synthetic and real data are presented to illustrate the application of the algorithm. The paper is organized as follows: Section II formulates the problem from a mathematical point of view and section III presents the experimental results. Section IV concludes the paper.

II. PROBLEM FORMULATION

The sequence under analysis, \mathbf{Y} , is the result of a FLIP experiment. Data can be represented by a 3D tensor, $\mathbf{Y} = \{y(i, j, t)\}$, containing a stack of L *fluorescence confocal*

Correspondent author: Isabel Rodrigues (irodrigues@isr.ist.utl.pt).

Partially supported by FCT, under ISR/IST pluriannual funding (POSC program, FEDER)

Affiliation: ¹Instituto Superior de Engenharia de Lisboa, ²Instituto de Sistemas e Robótica, ³Instituto Superior Técnico, Lisbon, Portugal

microscopy (FCM) images with $0 \leq i, j, t \leq N - 1, M - 1, L - 1$. Each image at the discrete time t_0 , $y(i, j, t_0)$, is corrupted by Poisson noise as well as each time course associated with the pixel (i_0, j_0) , $y(i_0, j_0, t)$. In this paper the image sequence corresponds to L observations of a cell nucleus along the time, acquired at a period rate of 30 seconds. The goal of this study is to estimate the underlying cell nucleus morphology, \mathbf{X} , from the noisy observed images, \mathbf{Y} , exhibiting a very low *signal to noise ratio* (SNR), as shown in Fig. 1.

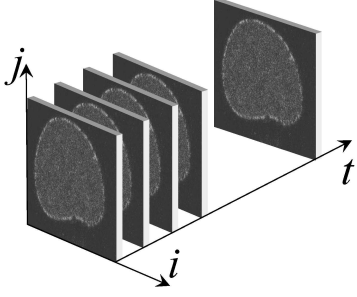


Fig. 1. Fluorescence confocal microscopy image sequence along the time.

A Bayesian approach is adopted to estimate \mathbf{X} by solving the following optimization problem

$$\hat{\mathbf{X}} = \arg \min_{\mathbf{X}} E(\mathbf{X}, \mathbf{Y}) \quad (1)$$

where the energy function is a sum of two terms, $E(\mathbf{X}, \mathbf{Y}) = E_Y(\mathbf{X}, \mathbf{Y}) + E_X(\mathbf{X}, \mathbf{Y})$. $E_Y(\mathbf{X}, \mathbf{Y})$ is called the *data fidelity term* and $E_X(\mathbf{X}, \mathbf{Y})$ is called the *prior term*. The first term pushes the solution toward the observations according to the type of noise corrupting the images and the prior term smooths the solution [6], [7]. If independence of the observations is assumed, the *data fidelity term* is defined as

$$E_Y(\mathbf{X}, \mathbf{Y}) = -\log \left[\prod_{i,j,t} p(y(i, j, t) | x(i, j, t)) \right]. \quad (2)$$

Since the images are corrupted by Poisson noise, $p(y|x) = \frac{x^y}{y!} e^{-x}$, the log data fidelity term is

$$E_Y(\mathbf{X}, \mathbf{Y}) = \sum_{i,j,t=0} d(i, j, t) + C \quad (3)$$

where C is a constant term and $d(i, j, t) = x(i, j, t) - y(i, j, t) \log(x(i, j, t))$.

The prior term regularizes the solution by removing the noise. Here an anisotropic prior term is used, in the sense that the penalization between neighboring pixels is one value for pixels at the same image (spatial correlation) and another for neighboring pixels from different images (time course correlation). The prior is a Gibbs distribution with *log-Euclidean* potential functions which are the more appropriated when the unknowns to be estimated are all positive [5], [8],

$$p(\mathbf{X}) = \frac{1}{Z} e^{-U(\mathbf{X})} \quad (4)$$

where

$$U(\mathbf{X}) = \alpha \left[\log^2 \left(\frac{x(i, j, t)}{x(i-1, j, t)} \right) + \log^2 \left(\frac{x(i, j, t)}{x(i, j-1, t)} \right) \right] + \beta \log^2 \left(\frac{x(i, j, t)}{x(i, j, t-1)} \right) \quad (5)$$

The prior term is $-\log E_X(\mathbf{X})$ and therefore the overall energy function to be minimized is

$$E(\mathbf{X}, \mathbf{Y}) = \sum_{i,j,t=0}^{N-1, M-1, L-1} [x(i, j, t) - y(i, j, t) \log(x(i, j, t))] + \alpha \sum_{i,j,y} \left[\log^2 \left(\frac{x(i, j, t)}{x(i-1, j, t)} \right) + \log^2 \left(\frac{x(i, j, t)}{x(i, j-1, t)} \right) \right] + \beta \sum_{i,j,y} \log^2 \left(\frac{x(i, j, t)}{x(i, j, t-1)} \right) \quad (6)$$

The minimization of this energy function (6) is not a convex problem and its optimization using the a *gradient descent* or Newton-Raphson based methods is difficult. However, performing an appropriate change of variable $z(i, j, t) = H(x(i, j, t))$, it is possible to turn it into convex. Let $z(i, j, t) = H(x(i, j, t)) = \log(x(i, j, t))$ or $x(i, j, t) = e^{z(i, j, t)}$. The function $H(x)$ is monotonic and therefore the minimizers of $E(\mathbf{X}, \mathbf{Y})$ and $E(\mathbf{Z}, \mathbf{Y})$ are related by $\mathbf{Z}^* = \log(\mathbf{X}^*)$. The new energy function becomes

$$E(\mathbf{Z}, \mathbf{Y}) = \sum_{i,j,t} \left[e^{z(i,j,t)} - y(i, j, t) z(i, j, t) \right] + \alpha \sum_{i,j,t} (z(i, j, t) - z(i-1, j, t))^2 + (z(i, j, t) - z(i, j-1, t))^2 + \beta \sum_{i,j,t} (z(i, j, t) - z(i, j, t-1))^2 \quad (7)$$

where α and β are prior parameters to tune the level of smoothing across the images and across the time courses respectively.

The minimization of (7) is performed by finding its stationary point according to the first order condition

$$\nabla E(\mathbf{Z}, \mathbf{Y}) = 0 \quad (8)$$

or

$$\frac{\partial E(\mathbf{Z}, \mathbf{Y})}{\partial z(i, j, t)} = e^{z(i, j, t)} - y(i, j, t) + 2h(i, j, t) \quad (9)$$

with

$$h(i, j, t) = \alpha [N_s z(i, j, t) - \sum_s z_s(i, j, t)] + \beta [N_t z(i, j, t) - \sum_\tau z_\tau(i, j, t)] \quad (10)$$

where $z_s(i, j, t)$ and $z_t(i, j, t)$ are the $N_s = 4$ spatial and $N_t = 2$ temporal neighbors of $z(i, j, t)$ respectively.

The tensor $\mathbf{H} = \{h(i, j, t)\}$ may be computed by

$$\mathbf{H} = \Phi * \mathbf{Z} \quad (11)$$

where $*$ denotes the 3D convolution and Φ is the following 3D mask

$$\Phi = \begin{pmatrix} 0 & 0 & 0 \\ 0 & -\beta/N_t & 0 \\ 0 & 0 & 0 \\ \hline 0 & -\alpha/N_s & 0 \\ -\alpha/N_s & \alpha N_s + \beta N_t & -\alpha/N_s \\ \hline 0 & -\alpha/N_s & 0 \\ 0 & 0 & 0 \\ 0 & -\beta/N_t & 0 \\ 0 & 0 & 0 \end{pmatrix}. \quad (12)$$

The solution of (8) is obtained by solving the following convex equation

$$F(\mathbf{Z}) = e^{\mathbf{Z}} - \mathbf{Y} + 2\Phi * \mathbf{Z} = \mathbf{0} \quad (13)$$

using the Newton-Raphson method

$$\mathbf{Z}^{(k+1)} = \mathbf{Z}^{(k)} - \frac{e^{\mathbf{Z}^{(k)}} - \mathbf{Y} + 2\Phi * \mathbf{Z}^{(k)}}{e^{\mathbf{Z}^{(k)}} + 2(\alpha N_s + \beta N_t)} \quad (14)$$

where k stands for the iteration number.

Reversing the change of variable, the final solution is

$$\hat{\mathbf{X}} = e^{\mathbf{Z}} \quad (15)$$

III. EXPERIMENTAL RESULTS

In order to quantize the quality of the denoising methodology described above, synthetic data were generated: a stack of 50 images, 55×80 pixels. The images are corrupted by Poisson noise with an intensity decreasing for each pixel following an exponential decay along the time. The synthetic images were processed using the denoising methodology described above. Fig. 2 shows the noisy ((a) and (c)) and denoised ((b) and (d)) synthetic images for two time instants in the sequence. The SNR (signal to noise ratio) were computed before and after denoising and the results for (a) and (b) were respectively 8.47 and 13.12 and for (c) and (d) were respectively 2.60 and 10.42, suggesting a substantial improvement in the quality of the images. Two time courses can be seen in Fig. 3. The right plot corresponds to a pixel in the bleached region where the SNR before and after the denoising procedure are 12.74dB and 14.37db respectively. The left plot represents the time course for a different pixel further away from the bleached region and the SNR before and after denoising are respectively 16.65dB and 25.15dB. These SNR results mean that the noise associated with lower intensities (inside the hole) is harder to remove than the noise connected with the higher ones. The global (3D) SNR improved is 1.66dB from 7.85dB to 9.51dB.

The sequence of real data under analysis, \mathbf{Y} , is the result of a FLIP experiment where a spot of 30 pixels diameter was repeatedly bleached at intervals of 3.63 s and imaged between 27 ms bleach pulses. From a series of 350, 90 images of 260×380 pixels are used for testing. The 3D tensor $\mathbf{Y} = \{y(i, j, t)\}$ represents the stack of *fluorescence confocal microscopy* (FCM) images with $0 \leq i, j, t \leq 259, 379, 89$ where no background was subtracted. The only

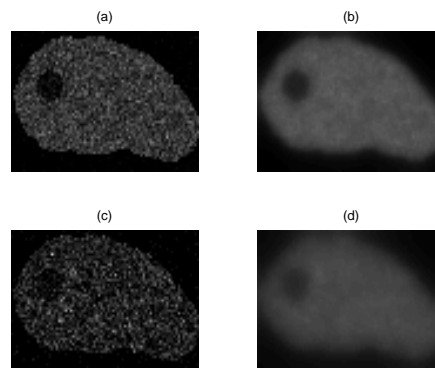


Fig. 2. Noisy (a) and (c) and denoised synthetic (b) and (d) data

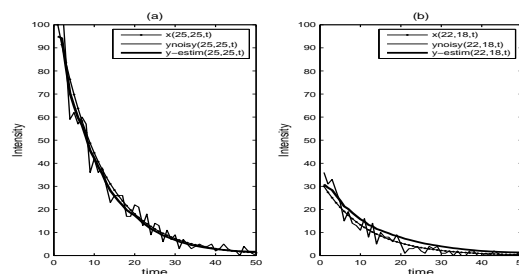


Fig. 3. Time courses for synthetic data outside the hole (a) and inside the hole (b)

preprocessing performed on the acquired data was a simple alignment procedure to correct for cell displacement during image acquisition, that consisted of a set of rigid body transforms driven by the maximization of the correlation between images.

In order to estimate \mathbf{X} , the aligned images were then processed using the denoising methodology described above. The CPU time of the algorithm was 1.2s *per* iteration in a Centrino Duo 2.00GHz, 1.99 GB RAM processor. The results for three images of the stack are shown in Fig. 4; images (a), (c) and (e) show the raw aligned cell nucleus data for $t = 5, 45, 85$; (b), (d) and (f) show the respective denoised images. As can be seen in these figures there is a great deal of improvement in the quality of the representation. The blur present in the denoised images results from the *log-quadratic* prior used to remove the noise. This undesirable effect may be attenuated by using other priors namely, edge preserving priors such as *total variation* (TV).

Improvements can also be noticed in the time dimension. Results for two time courses are shown in Fig. 5. Both plots show noisy and denoised time courses, the left one for pixel (136, 183) and the right one for pixel (105, 85), respectively outside and inside the bleached region.

A graph-cuts segmentation procedure was performed on the denoised data in order to display the propagation of the fluorescence loss that occurs inside the nucleus with time. The segmentation results for instants $t = 10, 75$ of the denoised images are shown in Fig. 6 (a) and (c); results

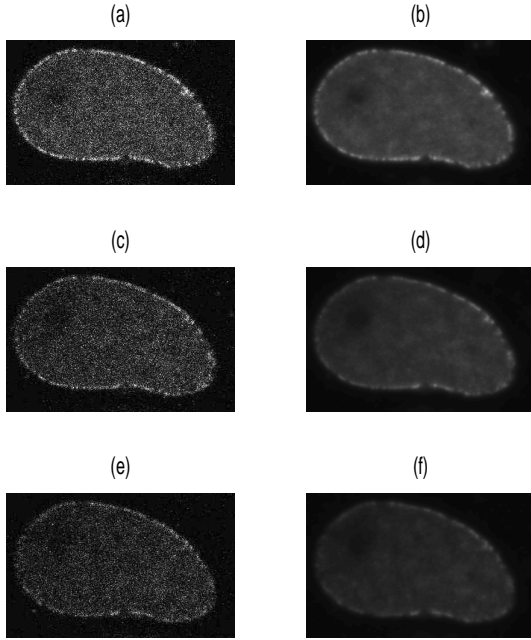


Fig. 4. Raw data and filtered data of HeLa immortal cell nucleus for $t=5, 50, 90$.

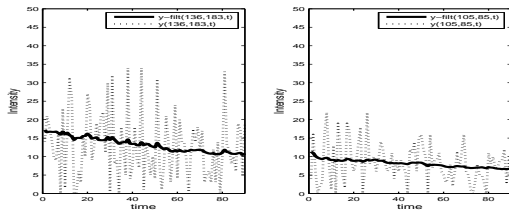


Fig. 5. Time courses outside the bleach region (a) and inside the bleached region (b).

for the companion segmentation can be seen in Fig. 6 (b) and (d). As shown in the figure, the fluorescence loss spreads inside the nucleus from a region around the bleached area toward the edges of the nucleus, particularly on the left side, since the bleach area is not standing in the center of the nucleus.

IV. CONCLUSIONS

In this paper a new denoising algorithm is proposed to *Fluorescence Confocal Microscopy* (FCM) imaging with *photobleaching*. The sequence of FCM images taken along the time, in this microscopy modality, are corrupted by a type of multiplicative noise described by a Poisson distribution. Furthermore, the global intensity of the images decreases along the time due to permanent fluorophore loss of its ability to fluoresce, caused by chemical reactions induced by the incident laser or by other surrounding molecules. The decreasing on the image intensity is "associated" to a decreasing on the signal to noise ratio of the images, making

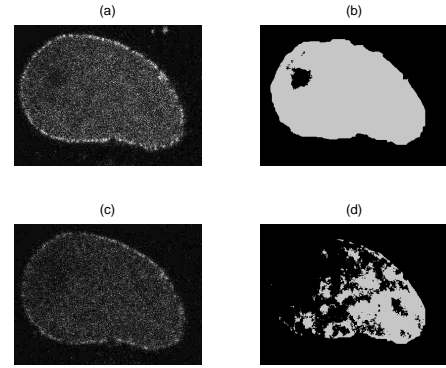


Fig. 6. Photobleaching propagation across the nucleus from the bleached area. Raw data (left) and segmentation results (right) for images $t = 10$ and $t = 75$.

the biological information recovery a difficult task [9].

In this paper a Bayesian algorithm is proposed to perform a simultaneous denoising procedure in the space (images) and in time (time course) dimensions. This approach, conceived as an optimization task with the *maximum a posteriori* (MAP) criterion, leads to a filtering formulation involving a 3D (2D+time) anisotropic filtering procedure. The energy function is designed to be convex and its minimizer is computed by using the Newton method which allows continuous convergence toward the global minimum, in a small number of iterations.

Tests using synthetic and real data have shown the ability of the methodology to reduce the multiplicative noise corrupting the images and the time courses.

V. ACKNOWLEDGMENT

The authors thank Dr. José Rino and Prof^a Maria do Carmo Fonseca, from the Molecular Medicine Institute of Lisbon, for providing biological technical support and the data used in this paper. We want also to thank Prof. João Xavier from the Systems and Robotics Institute, for his contributions to this paper.

REFERENCES

- [1] J. W. Lichtman and J. A. Conchello, "Fluorescence microscopy." *Nat Methods*, vol. 2, no. 12, pp. 910–9, 2005.
- [2] "Molecular expressions. optical microscopy primer." [Online]. Available: <http://micro.magnet.fsu.edu/primer/index.html>
- [3] J. Lippincott-Schwartz, N. Altan-Bonnet, and G. H. Patterson, "Photobleaching and photoactivation: following protein dynamics in living cells." *Nat Cell Biol*, vol. Suppl, September 2003. [Online]. Available: <http://view.ncbi.nlm.nih.gov/pubmed/14562845>
- [4] R. Underwood, "Frap and flip, photobleaching technique to reveal cell dynamics," 2007. [Online]. Available: http://www.nikoninstruments.com/images/stories/litpdfs/nikon_note_3nn06_8_07_lr.pdf
- [5] V. Arsigny, P. Fillard, X. Pennec, and N. Ayache, "Log-Euclidean metrics for fast and simple calculus on diffusion tensors," *Magnetic Resonance in Medicine*, vol. 56, no. 2, pp. 411–421, August 2006.
- [6] T. K. Moon and W. C. Stirling, *Mathematical methods and algorithms for signal processing*. Prentice-Hall, 2000.
- [7] J. M. Sanches and J. S. Marques, "Joint image registration and volume reconstruction for 3d ultrasound," *Pattern Recogn. Lett.*, vol. 24, no. 4–5, pp. 791–800, 2003.
- [8] S. Boyd and L. Vandenberghe, *Convex Optimization*. Cambridge University Press, March 2004.
- [9] N. A. M. A. Lashin, "Restoration methods for biomedical images in confocal microscopy," Ph.D. dissertation, Berlin, 2005.